THE JOURNAL OF PHYSICAL CHEMISTRY B

ARTICLE

pubs.acs.org/JPCB

Structural Relaxation in the Singlet Excited State of Star-Shaped Oligofluorenes Having a Truxene or Isotruxene as a Core

Mamoru Fujitsuka,[*,†] Dae Won Cho,[†,‡] Hsin-Hau Huang,[§] Jye-Shane Yang,[§,*] and Tetsuro Majima[*,†]

[†]The Institute of Scientific and Industrial Research (SANKEN), Osaka University, Mihogaoka 8-1, Ibaraki, Osaka 567-0047, Japan

[‡]Konkuk University-Fraunhofer ISE Next Generation Solar Cell Research Center (KFnSC), Konkuk University, Seoul, 143-701, Korea

[§]Department of Chemistry, National Taiwan University, Taipei, Taiwan 10617

Supporting Information

ABSTRACT: Oligofluorenes attract wide attention due to their excellent fluorescent properties. For the detailed understanding of the excited state properties, ultrafast processes have to be clarified. Here, we have investigated the structural relaxation in the singlet excited state of star-shaped oligofluorenes with a truxene or isotruxene core, to which oligofluorenes (n = 1−4) were attached. The transient absorption peak showed red-shift with time upon excitation. The fluorescence decay profiles in the picosecond domain showed the fast component in addition to the component corresponding to the singlet excited state lifetime. These ultrafast phenomena can be attributed to the structural relaxation, i.e., planarization, in the singlet excited state. The planarization process was supported by the theoretical calculation based on the time-dependent density functional theory. Furthermore, dependence of two-photon absorption cross section on the core of the star-shaped oligofluorene has been elucidated.

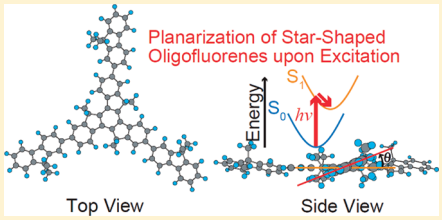

INTRODUCTION

Poly- and oligofluorenes have been intensively studied for years because of their high fluorescence quantum yield and high carrier mobility applicable to light emitting diode and so on.[1,2] Chemical modifications have been successfully carried out to realize high solubility, liquid crystallinity, chirality, and so on. To modify their properties useful to the applications, two-dimensional star-shaped systems seem to be attractive candidates.[3]

For construction of the star-shaped oligofluorenes, utilization of a truxene core, which can be regarded as overlapping three fluorene units with 3-fold symmetry, or an isotruxene core, an unsymmetrical isomer of truxene, is attractive because the oligofluorene backbone can be maintained through the core part. The syntheses of star-shaped oligofluorenes with a truxene or isotruxene core have been already reported.[4,5] Furthermore, their basic photochemical properties including steady state absorption and fluorescence properties have been also reported.[4−6] Especially high fluorescence quantum yield is an important characteristic of these star-shaped oligofluorenes.[4,5] For a detailed understanding of the excited state properties of these star-shaped molecules, information on the relaxation process such as structural relaxation in the excited state is indispensable.

In the present study, we have investigated the ultrafast relaxation process in the singlet excited state of the star-shaped oligofluorenes with a truxene or isotruxene core (TFn and ITFn, n = 1−4, Figure 1) by means of femtosecond laser spectroscopy. The relaxation process from the Franck−Condon state to the relaxed state was successfully observed with the transient absorption spectroscopy as well as fluorescence decay measurements using the fluorescence up-conversion technique. The observed relaxation process was assigned to the planarization process of the star-shaped oligofluorenes. The assignment was supported by the theoretical calculations based on the time-dependent density functional theory. Furthermore, dependence of two-photon absorption cross section on the core of the star-shaped oligofluorene was elucidated.

EXPERIMENTAL METHODS

Materials. A series of TFn and ITFn (n = 1−4, Figure 1) were synthesized according to the procedures reported in the previous papers.[4,5] In the present study, spectroscopic grade toluene or tetrahydrofuran (THF) was used as a solvent for the optical measurements.

Apparatus. The subpicosecond transient absorption spectra were measured by the pump and probe method using a regeneratively amplified titanium sapphire laser as reported previously.[7] In the present study, the sample was excited using a 360 or 400 nm laser pulse. The 360 nm laser pulse was generated by an optical parametric amplifier. The 400 nm laser pulse was the second harmonic generation of the fundamental.

The fluorescence decay profiles were measured by the single photon counting method using a streakscope.[8] The ultrashort laser pulse was generated by a Ti:sapphire laser (80 fs fwhm). For excitation of the sample, the output of the Ti:sapphire laser was converted to the second harmonic generation (360−400 nm)

Received: August 4, 2011
Revised: October 5, 2011
Published: October 10, 2011

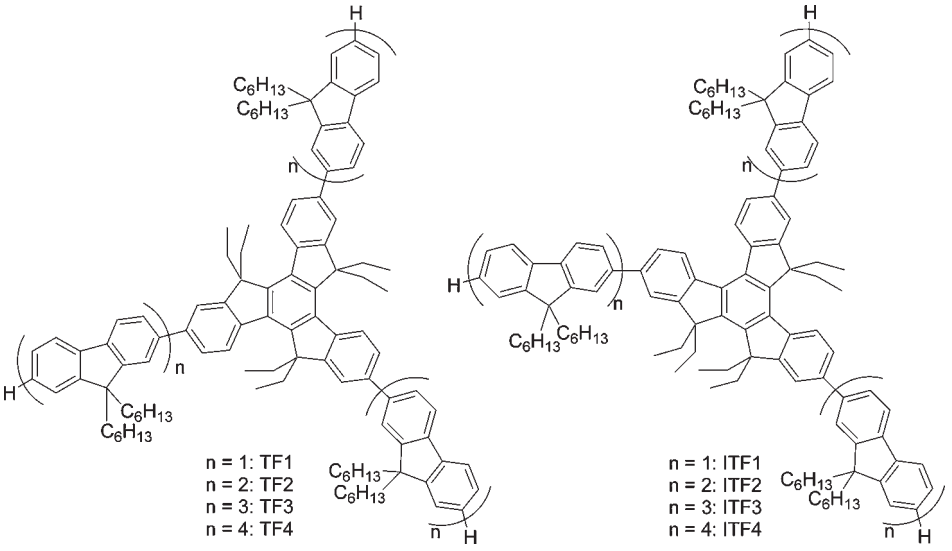

Figure 1. Molecular structures of truxene and isotruxene conjugated with oligofluorenes (TF*n* and ITF*n*, *n* = 1−4).

using a BBO crystal. The fluorescence decay profile in the subpicosecond to picosecond regions was measured by means of the fluorescence up-conversion method described in the previous paper.[7]

The steady state absorption and fluorescence spectra were measured using a Shimadzu UV-3100PC and Hitachi 850, respectively.

Two-photon absorption cross-section ($\sigma^{(2)}$) values were measured by the open aperture Z-scan method.[9] All the samples were 100−200 μM solutions in THF. The femtosecond laser beam from a Ti:sapphire regenerative amplifier system (Spectra-Physics, Spitfire Pro F, 1 kHz 800 nm, 130 fs fwhm) was divided into two parts. One was monitored by a photodiode as an intensity reference, and the other was used for transmittance measurement. After passing through an f = 10 cm lens, the laser beam was focused and passed through a quartz cell (1 mm). The position of the sample cell could be varied along the laser beam direction (z-axis). The transmitted laser beam from the sample cell was detected by a photoreceiver (New Focus, model 2031) and averaged by a gated integrator (Stanford Research Systems, SR250). Details of evaluation of the two-photon absorption cross section value were indicated in the Supporting Information (SI).

Theoretical Calculation. Optimized structures in the ground and excited states were estimated at B3LYP/6-31G(d) and time-dependent (TD) B3LYP/6-31G(d) levels, respectively, using the Gaussian 09 package.[10]

RESULTS AND DISCUSSION

Steady State Absorption and Fluorescence Properties. Figure 2 shows steady state absorption and fluorescence spectra of TF*n* and ITF*n* (*n* = 1−4) in toluene. Observed spectra are essentially the same as those reported in the previous papers.[4,5] TF*n* showed absorption and fluorescence peak shifts with an increase in the *n* value (Figure 2a). The observed shift can be attributed to the development of the π-conjugation system with the *n* value. In the case of ITF*n* (Figure 2b), although a similar peak shift was observed when the *n* value increased from 1 to 2, the red-shift observed with *n* = 2−4 was rather small. The red-shifted absorption and fluorescence maxima for ITF*n* vs TF*n* of the same *n* value have been attributed to stronger conjugation

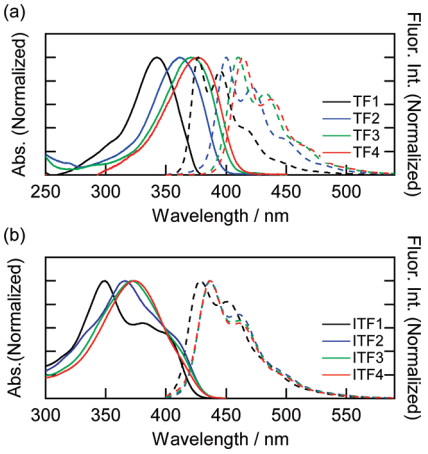

Figure 2. Normalized absorption (solid line) and fluorescence (dashed line) spectra of (a) TF*n* and (b) ITF*n* (*n* = 1−4) in toluene.

interactions among the oligofluorene arms through the ortho−para vs meta−meta connectivity.[5]

Fluorescence lifetimes of TF*n* and ITF*n* estimated by the single photon counting method were summarized in Table 1. For both TF*n* and ITF*n*, fluorescence lifetimes tend to become shorter with an increase in the *n* value. This tendency is the same as other oligomers including oligofluorenes and can be attributed to the larger oscillator strength of longer oligomers. Compared to TF*n*, the fluorescence lifetime of ITF*n* is slightly insensitive to an increase in the *n* value. For example, the ratios of fluorescence lifetime of *n* = 4 to *n* = 1 were estimated to be 0.24 and 0.68 for TF*n* and ITF*n*, respectively. The observed tendency is consistent with the *n* value dependence of absorption and fluorescence properties of TF*n* and ITF*n*, such as peak positions and so on.

Transient Absorption Spectra of the Singlet Excited State. Figure 3 shows transient absorption spectra of TF*n* (*n* = 1−4) in toluene during the laser flash photolysis using a femtosecond laser. Immediately after the laser excitation, each compound showed a transient absorption band in the region of 657−770 nm. The

dx.doi.org/10.1021/jp2074336 |J. Phys. Chem. B 2011, 115, 13502–13507

Table 1. Excitation Properties of TF*n* and ITF*n* (*n* = 1−4) in Toluene

	λ_{Sn-S1}/nm[a]	τ_{Sn-S1}/ns[b]	τ_{rel}^{abs}/ps	τ_{rel}^{fl}/ps	$\sigma^{(2)}$/GM[c]
TF1	655 (−)[d]	2.6 (2.49)	−[d]	23	183
TF2	734 (745)	0.69 (0.74)	30	23	251
TF3	761 (768)	0.65 (0.64)	25	25	292
TF4	770 (774)	0.55 (0.60)	27	27	399
ITF1	780−820 (−)[e]	1.0 (1.22)	−[e]	18	218
ITF2	780−820 (−)[e]	1.0 (0.97)	−[e]	15	297
ITF3	780−820 (−)[e]	0.73 (0.84)	−[e]	16	465
ITF4	780−820 (−)[e]	0.70 (0.83)	−[e]	16	797

[a] Peak position of the S_n-S_1 absorption at 10 ps after the laser excitation. Numbers in parentheses are $\lambda_{Sn-S1}(\infty)$ in the following equation: $\lambda_{Sn-S1}(t) = [\lambda_{Sn-S1}(\infty) - \lambda_{Sn-S1}(0)][1 - \exp(-t/\tau_{rel}^{abs})] + \lambda_{Sn-S1}(0)$, where $\lambda_{Sn-S1}(0)$ is λ_{Sn-S1} at $t = 0$. τ_{rel}^{abs} is the relaxation time constant. [b] Decay time constant of the S_n-S_1 absorption band. Numbers in parentheses are the fluorescence lifetime. [c] The $\sigma^{(2)}$ values were estimated using rhodamine 6G as a reference. See the Supporting Information for details. Solvent was THF. [d] Peak shift was not observed. [e] Transient absorption peak is difficult to see due to instrumental limitation.

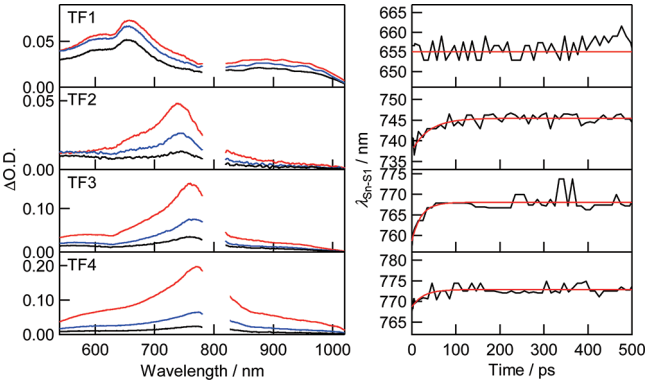

Figure 3. (Left) Transient absorption spectra of TF*n* (*n* = 1−4) in toluene at 10 (red), 500 (blue), and 1000 ps (black) after excitation during the laser flash photolysis using 360 (*n* = 1−3) or 400 nm (*n* = 4) femtosecond laser. (Right) Time-dependence of the peak position of S_n-S_1 absorption band (λ_{Sn-S1}).

transient absorption bands decayed according to the single exponential function. These transient absorption bands can be assigned to the singlet excited state because the decay lifetimes (τ_{Sn-S1}) are in good agreement with the corresponding fluorescence lifetimes as summarized in Table 1.

It was revealed that the peak position of S_n-S_1 absorption (λ_{Sn-S1}) of TF2, TF3, and TF4 tends to shift to the longer-wavelength side during the initial few tens of picoseconds after the laser excitation as indicated in the right panel of Figure 3. The time constant of the present peak shift (τ_{rel}^{abs}) was estimated using the equation indicated in the footnote of Table 1 to be 30, 25, and 27 ps for TF2, TF3, and TF4, respectively. It has been reported that oligofluorenes show a fluorescence peak shift to the longer-wavelength side due to torsional relaxation along the bond connecting two fluorene units.[11] The time constant of the torsional relaxation was reported to be 40 ps in solution at room temperature. Furthermore, the fluorescence peak shift in the initial $10-10^2$ ps due to the torsional relaxation, which results in

Scheme 1. Schematic Energy Diagram about the Relaxation Process in the Excited State as Well as the Top and Side Views[a]

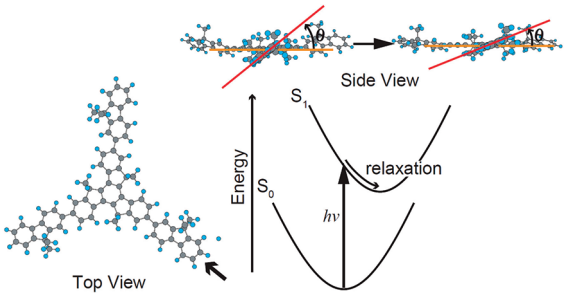

[a] An arrow in the top view indicates the view direction of the side view. In the side view, red and orange lines indicate core and fluorene planes, respectively.

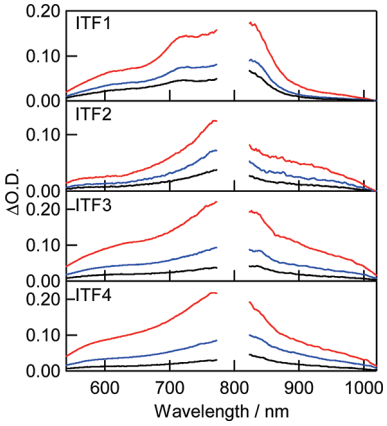

Figure 4. Transient absorption spectra of ITF*n* (*n* = 1−4) in toluene at 10 (red), 500 (blue), and 1000 ps (black) after excitation during the laser flash photolysis using a 400 nm femtosecond laser.

planarization of oligomer, in the excited state has been also reported for oligothiophenes.[12] The time constants observed with the present TF*n* are in good agreement with the former reported planarization time of other oligomers. Furthermore, planarization of fluorene units of TF*n* is expected to cause the enhancement of π-conjugation, which should result in a red-shift of the transient absorption band as well as fluorescence band. Therefore, the present spectral change of TF*n* can be attributed to the torsional relaxation of TF*n* upon excitation to the singlet excited state (Scheme 1). In the case of TF1, a spectral shift was not observed, while similar structural relaxation is expected for TF1. The absence of the transient absorption peak shift probably indicates that the transition dipole responsible for the absorption maximum of S_1-excited TF1 is different from others as suggested by the different spectral shape of the transient absorption of TF1 from others.

In the case of ITF*n*, the singlet excited state showed an absorption peak around 800 nm (Figure 4). Dependence of the peak position of the transient absorption band on the *n* value seems rather small. The peak position of the S_n-S_1 absorption was difficult to be determined using the present facility, in which white continuum probe light was generated using the fundamental of the Ti:sapphire amplifier (800 nm). Thus, analysis of

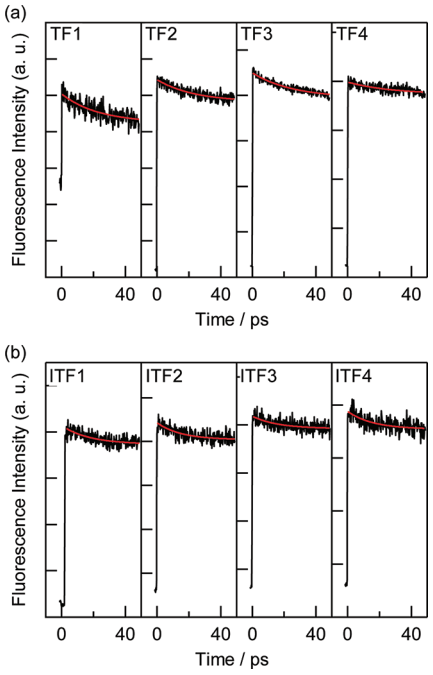

Figure 5. Fluorescence decay profiles of (a) TF*n* and (b) ITF*n* in toluene measured by fluorescence up-conversion. Excitation wavelength: TF1, 360 nm; TF2−4, 380 nm; ITF1−4, 400 nm. Observed wavelength: TF1, 380 nm; TF2, 400 nm; TF3,4, 420 nm; ITF1−4, 430 nm. Red line is fitted curve.

time dependence of the peak position of ITF*n* was impossible, although similar conformational relaxation to those of TF*n* is expected.

Structural Changes of TF*n* and ITF*n* Investigated by Fluorescence Up-Conversion. To investigate structural relaxation upon excitation to the singlet excited state furthermore, an ultrafast fluorescence decay profile was measured by using a fluorescence up-conversion technique because a fluorescence band is also sensitive to the structural change upon excitation. In Figure 5, fluorescence decay profiles of TF*n* and ITF*n* at the shorter-wavelength side of each fluorescence band are indicated. It is clear that each time profile exhibits a decay component, which cannot be fitted with the time constant corresponding to the singlet excited state lifetime (Table 1). On the other hand, the time profile of fluorescence measured at the longer-wavelength side of the fluorescence band showed a rise with the same time constant as that of decay observed at the shorter-wavelength side (Figure S1 in SI), indicating the red-shift of the fluorescence band within the picosecond time domain. Therefore, the fast decay component observed in Figure 5 can be attributed to the structural relaxation from the Franck−Condon state to the relaxed singlet excited state as discussed in the former section. The time constant of the fast decay component (τ_{rel}^{fl}) was summarized in Table 1. In the cases of TF*n* (n = 2−4), the estimated values showed good agreement with the τ_{rel}^{abs} values estimated from the transient absorption peak shift. In the case of TF1, the fast component due to structural relaxation was observed, indicating that the transition dipole for the fluorescence may be along with the direction, to which planarization affects. Furthermore, the observation of the fast decaying component of ITF*n* supports the existence of the structural relaxation upon excitation, which could not be observed with transient absorption spectroscopy as indicated above. The τ_{rel}^{fl} values of ITF*n* are similar to those of TF*n*. For both TF*n* and ITF*n*, the relaxation time does not vary significantly with the *n* value.

Theoretical Calculation on the Planarization Process. To obtain further insight into the structural relaxation upon excited state formation, molecular structure in the ground state and the singlet excited state was estimated by molecular orbital calculation using the density functional theory at B3LYTP/6-31G(d) and TD B3LYP/6-31G(d) levels, respectively. For the simplicity of the calculation, the alkyl groups were reduced to the methyl groups. The calculation was carried out for TF1 and ITF1 in all anti- and syn-forms because it is well-known that various oligomers of cyclic aromatic compounds possess minima at both anti- and syn-forms. The designation of syn and anti refers to the orientation of the ring-bridged saturated carbons in the core vs the neighboring fluorene. In Figure 6, changes in the molecular structure, i.e., bond length and dihedral angle, upon the formation of the singlet excited TF1 in syn-form were indicated, as a representative. The results of the calculations on anti-form TF1 and anti- and syn-form ITF1 as well as those of the fluorene dimer were indicated in Figures S2−S5 in SI. In the case of anti-form TF1, several attempts for optimization at the TD-B3LYP/6-31G(d) level failed. Thus, the result at the TD-B3LYP/STO-3G level is shown in Figure S3 (SI). In these figures positive and negative changes were indicated by black and red, respectively.

In the case of syn-form TF1 (Figure 6), relatively larger bond length changes were observed with the central truxene core. Bond length changes of peripheral fluorene units are smaller when compared to those of the central core. Upon excitation, fluorene units showed an enhanced quinoid character. Furthermore, the bond connecting the core and the fluorene unit tends to become shorter, and both core and fluorene units become coplanar as evident from the dihedral angle (θ) formed by them. These results indicate that TF1 tends to become planar in the singlet excited state, i.e., planarization, supporting the identification of observed transient spectral change and fast component of fluorescence decay measured by the up-conversion method. The planarization upon excitation to the singlet excited state can also be observed with anti-form TF1 and syn- and anti-form ITF1. In the cases of syn- and anti-form TF1, structural changes are symmetrical due to the higher symmetrical structure of the core. On the other hand, structural changes in ITF1 are slightly unsymmetrical.

In Figure S2 in the SI, structural changes of the fluorene dimer upon excitation are also indicated. It is clear that the structural changes of the fluorene dimer are larger when compared to those of TF1 and ITF1. For example, the bond connecting two fluorene units becomes shorter by 0.047 Å, and the bond rotates 24.5° (θ: 142.0° → 166.4°) upon excitation. Corresponding values of syn-form TF1 are 0.016 Å and 9.7° (θ: 143.1° → 152.8°), indicating that the larger aromatic system seems to diminish substantial structural change by delocalization of the excited state over a larger aromatic system. Thus, in spite of the larger hydrodynamic volume, the smaller structural change of the larger star-shaped oligofluorene seems to make relaxation time similar to that of smaller star-shaped oligofluorene as observed in the experiments. The smaller structural change of larger star-shaped oligofluorene was also indicated from the transient absorption peak shift: For the TF2, TF3, and TF4, the peak shift of the transient absorption band was evaluated to be 25, 15, and 8 meV, respectively.

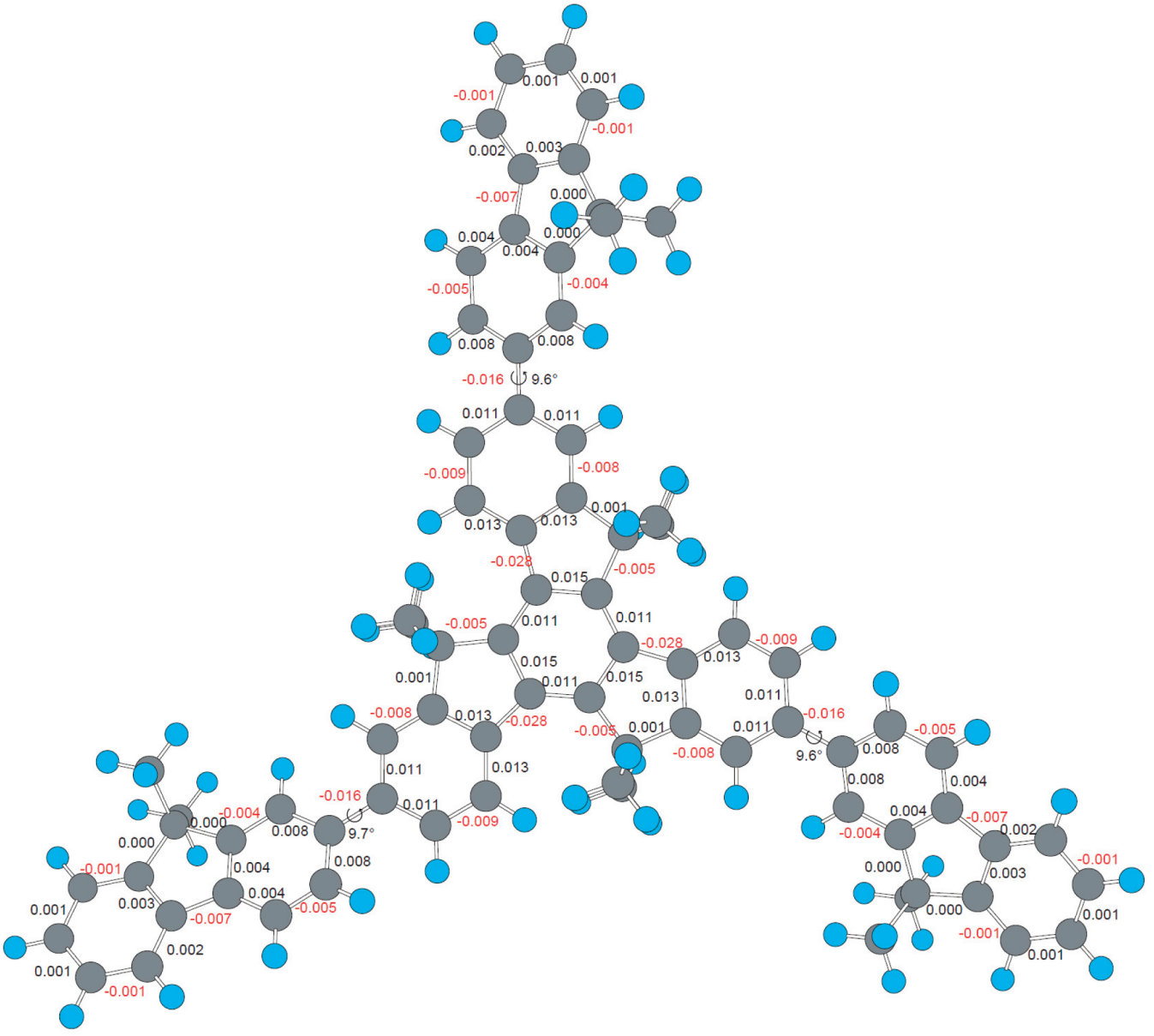

Figure 6. Structural (bond length (Å) and dihedral angle) changes of TF1 in all-syn-form upon excitation to the singlet excited state. The molecular structures in the ground and singlet excited states were calculated at B3LYP/6-31G(d) and TD-B3LYP/6-31G(d) levels, respectively. The dihedral angle between the planes formed by the truxene core and fluorene was defined to be 0° when fluorene and the core take an anti-form.

Two-Photon Absorption. In the former sections, the singlet excited states were generated by a single photon process, while generation by the two-photon process is also possible. Figure 7 shows a transmittance change of ITF4 in THF during Z-scan using an 800 nm femtosecond laser. By applying the procedure summarized in the SI, the two-photon absorption cross section ($\sigma^{(2)}$) value of ITF4 was estimated to be 797 GM. The $\sigma^{(2)}$ values of other TF*n* and ITF*n* were estimated as summarized in Table 1. For both TF*n* and ITF*n*, the $\sigma^{(2)}$ value increases with the *n* value, indicating the effect of the expanded π-conjugation system in two-photon absorption cross section. The $\sigma^{(2)}$ value of ITF*n* is larger than TF*n* for the same *n* value. This might reflect the importance of conjugation interactions among the oligofluorene arms, which is larger in ITF*n* than TF*n*,[5] in determining the $\sigma^{(2)}$ value of two-dimensional π-conjugated systems. Furthermore, the

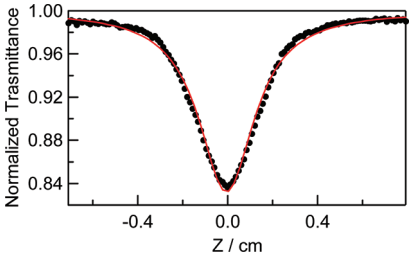

Figure 7. Normalized transmittance of ITF4 in THF during Z-scan using an 800 nm femtosecond laser.

$\sigma^{(2)}$ value of ITF*n* increases significantly with increasing *n* value. For example, for ITF*n*, 3.7 times an increase in the $\sigma^{(2)}$ value was

dx.doi.org/10.1021/jp2074336 |J. Phys. Chem. B 2011, 115, 13502–13507

observed when the *n* value was increased from 1 to 4, while the corresponding value for TF*n* is 2.2. The difference in the observed generation dependence of the $\sigma^{(2)}$ value may indicate that the molecular orbitals responsible for the two-photon absorption phenomena also depend on the symmetry of star-shaped oligofluorenes.

CONCLUSIONS

In the present paper, we have investigated the structural relaxation process in the singlet excited state of star-shaped oligofluorenes with a truxene or isotruxene core. The transient absorption and fluorescence decay profiles showed the fast component due to structural relaxation from the Franck−Condon state to the relaxed state of the singlet excited state. The relaxation process observed can be attributed to the planarization process, which was also supported by the theoretical calculation based on the time-dependent density functional theory. Furthermore, a larger two-photon absorption cross section was observed for the isotruxene-cored than for the truxene-cored systems.

ASSOCIATED CONTENT

Supporting Information. Details of evaluation of two-photon absorption cross section value, fluorescence profiles of TF3, and theoretical calculations of TF1, ITF1, and dimer of fluorene. This material is available free of charge via the Internet at http://pubs.acs.org.

AUTHOR INFORMATION

Corresponding Author

*E-mail address: fuji@sanken.osaka-u.ac.jp; jsyang@ntu.ed.tw; majima@sanken.osaka-u.ac.jp.

ACKNOWLEDGMENT

This work has been partly supported by a Grant-in-Aid for Scientific Research (Project 21350075, 22245022, Priority Area (477), and others) from the Ministry of Education, Culture, Sports, Science and Technology (MEXT) of Japanese Government. T.M. thanks the WCU (World Class University) program through the National Research Foundation of Korea funded by the Ministry of Education, Science and Technology (R31-10035) for the support. JSY thanks the National Science Council of Taiwan, ROC, for financial support.

REFERENCES

(1) (a) Leclerc, M. *J. Polym. Sci., Part A: Polym. Chem.* **2001**, *39*, 2867–2873. (b) Pogantsch, A.; Wenzl, F. P.; List, E. J.; Leising, G.; Grimsdale, A. C.; Mullen, K. *Adv. Mater.* **2002**, *14*, 1061–1064. (c) Kulkami, A. P.; Jenekhe, S. A. *Macromolecules* **2003**, *36*, 5285–5296. (d) Gruber, J.; Li, R. W. C.; Aguiar, L. H. J. M. C.; Benvenho, A. R. V.; Lessmann, R.; Hummelgen, I. A. *J. Mater. Chem.* **2005**, *15*, 517–522.

(2) Belletete, M.; Ranger, M.; Beaupre, S.; Mario, S.; Durocher, G. *Chem. Phys. Lett.* **2000**, *316*, 101–107.

(3) (a) Kanibolotsky, A. L.; Perepichka, I. F.; Skabara, P. J. *Chem. Soc. Rev.* **2010**, *39*, 2695–2728. (b) Detert, H.; Lehmann, M.; Meier, H. *Materials* **2010**, *3*, 3218–3330.

(4) Kanibolotsky, A. L.; Berridge, R.; Skabara, P. J.; Perepichka, I. F.; Bradley, D. D. C.; Koegerg, M. *J. Am. Chem. Soc.* **2004**, *126*, 13695–13702.

(5) (a) Yang, J.-S.; Lee, Y.-R.; Yan, J.-L.; Lu, M.-C. *Org. Lett.* **2006**, *8*, 5813–5816. (b) Yang, J.-S.; Huang, H.-H.; Ho, J.-H. *J. Phys. Chem. B* **2008**, *112*, 8871–8878. (c) Yang, J.-S.; Huang, H.-H.; Lin, S.-H. *J. Org. Chem.* **2009**, *74*, 3974–3977.

(6) Omer, K. M.; Kanibolotsky, A. L.; Skabara, P. J.; Perepichka, I. F.; Bard, A. J. *J. Phys. Chem. B* **2007**, *111*, 6612–6619.

(7) Fujitsuka, M.; Cho, D. W.; Tojo, S.; Inoue, A.; Shiragami, T.; Yasuda, M.; Majima, T. *J. Phys. Chem. A* **2007**, *111*, 10574–10579.

(8) Fujitsuka, M.; Okada, A.; Tojo, S.; Takei, F.; Onitsuka, K.; Takahashi, S.; Majima, T. *J. Phys. Chem. B* **2004**, *108*, 11935–11941.

(9) Sheik-Bahae, M.; Said, A. A.; Wei, T.-H.; Hagan, D. J.; Van Stryland, E. W. *IEEE J. Quantum Electron.* **1990**, *26*, 760–769.

(10) Frisch, M. J.; Trucks, G. W.; Schlegel, H. B.; Scuseria, G. E.; Robb, M. A.; Cheeseman, J. R.; Scalmani, G.; Barone, V.; Mennucci, B.; Petersson, G. A. et al. *Gaussian 09*, Revision A. 02; Gaussian, Inc.: Wallingford CT, 2009.

(11) (a) Dias, F. B; Maçanita, A. L.; de Melo, J. S.; Burrows, H. D.; Günter, R.; Scherf, U.; Monkman, A. P. *J. Chem. Phys.* **118**, *15*, 7119–7126. (b) Hitschich, S. I.; Dias, F. B.; Monkman, A. P. *Phys. Rev. B* **2006**, *74*, 045210.

(12) Wong, K. S.; Wang, H.; Lanzani, G. *Chem. Phys. Lett.* **1998**, *288*, 59–64. (b) Westenhoff, S.; Beenken, W. J. D.; Friend, R. H.; Greenham, N. C.; Yartsev, A.; Sundström, V. *Phys. Rev. Lett.* **2006**, *97*, 166804.